

2/14/05

**Simulation of Water Sources and Precipitation Recycling for the
MacKenzie, Mississippi and Amazon River Basins**

Michael G. Bosilovich *

and

Jiun-Dar Chern

NASA/Global Modeling and Assimilation Office

Code 610.1 Goddard Space Flight Center

Greenbelt MD

Submitted to J. Hydrometeorology

* *Corresponding address:* Global Modeling and Assimilation Office, Code 610.1, NASA Goddard Space Flight Center, Greenbelt, MD 20771, Michael.Bosilovich@nasa.gov

Simulation of Water Sources and Precipitation Recycling for the MacKenzie, Mississippi and Amazon River Basins

ABSTRACT

An atmospheric general circulation model simulation for 1948-1997 of the water budgets for the MacKenzie, Mississippi and Amazon River basins is presented. In addition to the water budget, we include passive tracers to identify the geographic sources of water for the basins, and the analysis focuses on the mechanisms contributing to precipitation recycling in each basin. While each basin's precipitation recycling has a strong dependency on evaporation during the mean annual cycle, the interannual variability of the recycling shows important relationships with the atmospheric circulation. The MacKenzie River basin has only a weak interannual dependency on evaporation, where the variations in zonal moisture transport from the Pacific Ocean can affect the basin water cycle. On the other hand, the Mississippi River basin has strong interannual dependencies on evaporation. While the precipitation recycling weakens with increased low level jet intensity, the evaporation variations exert stronger influence in providing water vapor for convective precipitation at the convective cloud base. High precipitation recycling is also found to be partly connected to warm SSTs in the tropical Pacific Ocean. The Amazon River basin evaporation exhibits small interannual variations, so that the interannual variations of precipitation recycling are related to atmospheric moisture transport from the tropical south Atlantic Ocean. Increasing SSTs over the 50-year period are causing increased easterly transport across the basin. As moisture transport increases, the Amazon precipitation recycling decreases (without real time varying vegetation changes). In addition, precipitation recycling from a bulk diagnostic method is compared to the passive tracer method used in the analysis. While the mean values are different, the interannual variations are comparable between each method. The methods also exhibit similar relationships to the terms of the basin scale water budgets.

1. Introduction

When analyzing water cycle intensity, regional variations can be significantly different from the global background (e.g. Bosilovich et al., 2005). The changes in precipitation can be very different over continents than global or oceanic changes. Precipitation over land is a function of both transport of water from the oceans and the evaporation from the land (Trenberth, 2003). The water holding capacity of the vegetation and soil limits land evaporation. Therefore, variations of the land evaporation can affect the surface energy budget, planetary boundary layer and the convective potential energy of the atmospheric column (Betts, 2004), and ultimately the feedback with precipitation. Persistence of soil moisture anomalies can lead to prolonged variations in the regional intensity of the water cycle (e.g. droughts or floods, Schubert et al. 2004a and b). The regional intensity of the water cycle can be quantified by calculating the local precipitation recycling (Brubaker et al., 1993; Eltahir and Bras, 1996; Dirmeyer and Brubaker, 1999; Bosilovich and Schubert 2001 and 2002; Stohl and James 2004; Yoshimura et al. 2004). Precipitation recycling is defined as the “contribution of local evaporation to local precipitation”, specifically delineating the source of mass of water in precipitation between local and remote geographic sources (Eltahir and Bras, 1996). This can be used to characterize and quantify the intensity of the regional water cycle.

Two recent studies provide the impetus for the numerical experiment presented here. Brubaker et al. (2001) showed the long-term analysis of evaporative sources for the Mississippi River Basin (MRB). Variations of evaporative oceanic sources can affect the recycling of precipitation. In addition, over 36-years some significant trends in sources of water for the basin were identified. Secondly, Bosilovich et al. (2005) evaluated climate atmospheric general circulation model (AGCM) simulations for 50-years duration. The AGCMs show global increasing trends of precipitation, but the trend of precipitation over land was decreasing. The

regional trends of precipitation differed in sign, magnitude and statistical significance. The regional evaluation of water cycle intensity, and the influence of local and large-scale processes were not investigated.

To better understand regional water cycles and the local influences and the atmospheric circulation variations on precipitation recycling, we have run a 50-year AGCM simulation (with prescribed SSTs), including diagnostics for the geographical sources of water vapor and precipitation recycling. In this paper, we focus on the water sources and precipitation recycling for the Global Energy and Water cycle Experiment (GEWEX) Continental-scale Experiments (CSEs) in the Americas (Figure 1). The MacKenzie GEWEX Study (MAGS) represents a high latitude basin. The Mississippi River Basin (MRB) is a mid-latitude basin with crucial agricultural production in the world economy (included in the GEWEX Americas Prediction Project, GAPP CSE). The Large-scale Biosphere Atmosphere experiment for the Amazon (LBA) is a tropical region where the local water cycle represents a substantial fraction of the globe, and where precipitation recycling has been studied for a long time. While other basins in Europe and Asia are equally important, these three represent a subset of different climate regimes for comparison.

2. Model and Methodology

a. Finite Volume General Circulation Model (fvGCM)

The atmospheric numerical model used in this study is the Finite Volume General Circulation Model (fvGCM; Lin, 2003). The finite-volume dynamical core uses a terrain-following Lagrangian control-volume vertical coordinate system (Lin 2003; Collins et al. 2003). The fvGCM dynamical core includes a conservative semi-Lagrangian transport algorithm. The algorithm has consistent and conservative transport of air mass and absolute vorticity (Lin and

Rood 1997). This feature of the system makes the fvGCM particularly useful for water vapor and passive tracer simulations.

The physical parameterizations of the fvGCM are based on NCAR Community Climate Model version 3.0 (CCM3) physics. The NCAR CCM3 parameterizations are a collection of physical processes with a long history of development and documentation (Kiehl et al. 1998). The moist physics package includes the Zhang and McFarlane (1995) deep convective scheme, which handles updrafts and downdrafts and operates in conjunction with the Hack (1994) mid- and shallow convection scheme. Bosilovich et al. (2003) validate regional aspects of the simulated hydrological cycle. This version of the fvGCM uses the Common Land Model (versions 2, described by Dai et al. 2003; Oleson et al. 2004). Bonan et al. (2002) and Zeng et al. (2002) evaluate the implementation of the CLM in the NCAR community GCM.

b. Precipitation Recycling

The model also includes water vapor tracers (WVT) to quantify the geographical source of water for global precipitation (Bosilovich and Schubert, 2002; Bosilovich 2002; Bosilovich et al. 2003). In this configuration, the source of water for a tracer is the evaporation from a predefined region (e.g. Figure 1). This humidity is then predicted as a passive tracer (separate and distinct from the model's specific humidity prognostic variable) including tracer transport and precipitation and turbulent tendencies, using

$$\frac{\partial q_T}{\partial t} = -\nabla_3 \cdot (q_T V) + \frac{\partial q_T}{\partial t}_{turb} + \frac{\partial q_T}{\partial t}_{Prec} \quad (1)$$

where q_T is the three-dimensional water vapor tracer, V is the three-dimensional wind, $turb$ denotes the turbulent tendency not including surface evaporation (vertically integrates to zero) and $Prec$ denotes the sum of all tracer precipitation tendencies (including condensation, rain evaporation, and convective vertical movement; vertically integrates to $-P_T$). The tracer

precipitation tendencies are computed proportional to the total precipitation tendency, where the proportionality is based on the ratio of tracer water to total water (Bosilovich and Schubert, 2002).

The WVT methodology requires a modest investment in developing the code and also computing additional atmospheric prognostic variables. Precipitation recycling (but not specific external sources) can also be determined by simpler bulk diagnostic methods (e.g. Brubaker et al. 1993). The bulk diagnostic methods use monthly data and solve a regional water budget. This can be compared to the value determined from the WVT method.

c. Experimental Design

The model simulation is evaluated for 50 years, from the beginning of 1948 through the end of 1997. Hadley Centre SSTs provide the prescribed oceanic boundary conditions for the AGCM (Rayner et al. 1996 and 2003). The experiment is similar to the first phase of the Climate of the Twentieth Century study (Folland et al. 2002) in that it uses prescribed SST variations, but not aerosols, carbon cycle, or other climate change input forcing (e.g. vegetations cover). The spatial resolution of the model grid is 2 degrees latitude by 2.5 degrees longitude. The initial conditions were derived from a longer simulation (started in 1901), and tracers were initialized at zero in September 1947. A total of 36 water vapor tracers (WVT) were defined by geographic location (Figure 1 only shows those relevant to the regional analysis discussed here). The basin areas were defined by interpolating the mask used by Roads et al. (2002) to the model's grid. The tracers are spun up within weeks of initialization (Bosilovich and Schubert, 2002).

3. Simulated Seasonal Cycle

Figure 2 compares the seasonal variations of precipitation of the model with the merged GPCP product (Adler et al. 2003) for the region of this investigation. The model produces large-scale convergent and divergent patterns that can be identified by the precipitation field. Over

the domain, there is an overestimate of precipitation. The most noticeable overestimates occur off the west coast of Central America in SON and DJF. Despite this, it is interesting to note that model seems to underestimate precipitation in the easternmost region of the Intertropical Convergence Zone (ITCZ) during JJA. The simulated precipitation across North America in JJA seems comparable to the merged data product. However, there appears to be an overestimate of precipitation in the northwestern quadrant of the Amazon River basin during SON.

Similarly, the comparison of simulated total precipitable water (TPW) with observations developed by NASA's Water Vapor Project (NVAP, Simpson et al. 2001) show that the model can reproduce the large-scale patterns (Figure 3). During SON, the model is wetter than observed over the Amazon basin, while the tropical Atlantic is drier than the NVAP data. The model simulated TPW over North America during JJA seems reasonable, especially in the regions of MAGS and MRB. There is a dry bias in the simulation over the Rocky Mountains. In general, the model simulated water cycle data seems reasonable, and we will consider potential impact of the regional biases on the results of analysis presented in subsequent sections.

In this paper, we will investigate the local influences and atmospheric circulation variations on precipitation recycling in MAGS, MRB and LBA. To simplify the analysis, we will focus on the three-month period of maximum precipitation recycling in each basin. Figure 4 shows the basin averaged major sources of precipitation for each basin. It should be noted that the number of sources for each region is generally a function of the configuration of the source regions (Figure 1). For example, MAGS has 4 primary sources of water vapor, likely because the North Pacific Ocean (NPO) is not discretized into smaller geographic regions. Consider that when the source (in the figure legends) is the same as the destination (Figure 4 a, MAGS; b, MRB; c, LBA), the curve is the basin precipitation recycling. The MAGS seasonal cycle is straightforward, where the Pacific Ocean sources dominate in winter, giving way to continental

sources in summer. The three month period of maximum precipitation recycling is May, June and July (MJJ). The size of a region also plays a role in the calculation of a water source; for example, the Asia (ASA) source of water for MAGS reaches a peak JJA because the continental evaporation is highest in Asian continent seasonal cycle.

For the MRB, we have discretized the tropical Atlantic ocean sources further, because of many questions regarding the impact of the Gulf of Mexico and Caribbean Sea on the climate of the United States. The MRB seasonal cycle is somewhat more complicated in that the maximum of precipitation recycling occurs during a transition from winter and early spring Pacific Ocean sources to fall tropical Atlantic sources. However, it is a clear annual cycle of precipitation recycling with a maximum in MJJ. Precipitation recycling in LBA (Figure 4c) is complicated by the lack of a clear seasonal cycle. While there is a distinct maximum during the onset season of October, November and December (OND), a rather high plateau exists from January to February (the wet season). The amount of recycled precipitation is also largest in OND, so we will focus on that time frame for intercomparing with MRB and MAGS.

4. Regional Water Budgets

The analysis of the model simulation from this point onward focuses on the seasons of maximum precipitation recycling for MAGS (MJJ), MRB (MJJ) and LBA (OND). In this section we evaluate the mean moisture budgets, including the geographical sources of water in the seasonal precipitation, and also the working relationships between the terms of the water budgets, precipitation recycling and external sources of water. In the following section, we extend this analysis to intercompare local and external forcing on the atmospheric circulation effects on precipitation recycling.

a. *MacKenzie River Basin*

Table 1 shows the basin and time averaged water balance quantities for the three basins being considered. In MAGS, evaporation is slightly larger than precipitation, but the primary transport of water vapor is zonal, and the rate of water flux at the zonal boundaries is much more than the average precipitation and evaporation. Almost 20% of the water precipitating in this season has come from evaporation (0.37 mm day^{-1}), so that 17% of evaporation stays in the basin, while the rest is transported out. This is slightly lower than the value computed with reanalysis (25%) by Szeto (2002). However, that value is computed by the Eltahir and Bras (1994) bulk diagnostic method, which has also been higher in other intercomparisons (Bosilovich and Schubert, 2002).

Even though this is the season where precipitation recycling is maximized in MAGS, the amount of water from the Pacific Ocean almost doubles the local source (Table 2), concurrent with the moisture transport through the western boundary of the basin. However, other land areas including the rest of Canada and even Asia, also provide significant sources of water. It is important to note that, in the current framework, we cannot more clearly identify source regions beyond the boundaries in Figure 1.

In order to better understand the mechanisms by which precipitation recycling occurs, we computed temporal correlations (from the time series of seasonal means for the 50 years of simulation) between the water budget terms and the WVTs (Table 3). Here, we see that the MAGS source for MAGS precipitation (e.g. the precipitation recycling ratio) correlates to precipitation at 0.53, but not as much to evaporation at 0.31. The correlation of recycling ratio to convective precipitation is higher (0.73, not in Table 3). It is interesting to note that the correlations of precipitation to the Pacific Ocean and Asia sources are negative. This indicates that when precipitation is high the recycling is high and the external sources are low. The zonal

moisture transport also reflects this feature. Given the lack of correspondence between evaporation and precipitation recycling, it appears that the moisture transport variations govern the precipitation recycling. Another issue not included in these tables is the impact of snow on the land-atmosphere interactions in MAGS. Snow is still present in this simulation, and is also observed, during May and June (Betts et al. 2003; MacKay et al. 2003). While snow does not show a clear relationship with precipitation recycling, snow does act to decrease the basin evaporation (correlation = -0.71, not shown in these tables). It seems that the partial presence of snow in space and time during this season could affect the precipitation recycling, but the interactions are not linear or spatially representative of the whole basin.

b. Mississippi River Basin

The Mississippi River Basin (MRB) has some similarities with MAGS, regarding the water budget. The maximum recycling season is MJJ in both cases. Also, both have mean evaporation only a small amount greater than the precipitation in this season (Table 1). Being further south, the MRB TPW is somewhat larger than MAGS, and the convective precipitation is much greater (93% of total precipitation in MRB is convective, compared to 74% in MAGS). The moisture transport from the south boundary is the dominant inflow of atmospheric water. The western boundary transport certainly contributes to the basin scale water cycle. The dominant sources of water for the MRB are from the tropical Atlantic Ocean regions (Table 2). While we have disaggregated these sources (including the Gulf of Mexico, Caribbean Sea and Tropical Atlantic Ocean), their combination exceeds the precipitation recycling (also, Brubaker et al. 2001). In many meteorological analyses, it is often noted that rain is occurring because of water from the Gulf of Mexico, when wind flows from the south across the south eastern United States. Given the differences in area extent, it is not surprising that the tropical Atlantic Ocean provides more moisture for precipitation than the Gulf of Mexico itself. The dominant oceanic

source is then the moist air mass that extends eastward back to Africa. Also, given the area extent of the Pacific Ocean source, it still makes a substantial contribution to the MRB water budget in MJJ.

The variability of the MRB water budget contrasts MAGS in several key relationships. Most notably, the precipitation and evaporation are highly correlated. Indeed, the precipitation recycling ratio is also highly correlated with both precipitation and evaporation. Bosilovich and Schubert (2001) evaluated the bulk diagnostic precipitation recycling for the central United States in the GEOS1 reanalysis, and found less sensitivity to evaporation. That system used prescribed soil moisture input, such that the evaporation could not respond to precipitation. Despite being the largest mean source of water for the MRB, the tropical Atlantic Ocean sources variability does not strongly correlate with total precipitation. Total precipitable water does positively correlate with northward transport of water through the south boundary. With the long distance that water has to travel from the tropical Atlantic to the MRB, the NTA water is mixing throughout the column. Surface evaporation, on the other hand, enters the atmosphere within the PBL and near the cloud base, so that it can be entrained into convection (e.g. Bosilovich 2002). Many models show that the central United States is a region where the coupling strength between the land and atmosphere is strong (Koster et al. 2004). The precipitation recycling may be another diagnostic of the land atmosphere coupling.

c. Amazon River Basin

Precipitation recycling has been considered an important feedback mechanism in the Amazon River basin for some time (Lettau et al. 1979; Eltahir and Bras, 1994). The Amazon basin differs substantially from MAGS and MRB, aside from the tropical geographic location. In this experiment, the precipitation and evaporation are much larger than the other basins. Also, precipitation is much more than the evaporation area averaged in the Amazon basin. The

simulated precipitation does exceed the GPCP estimates (Figure 2); though, basin averaged precipitation measurements can be approximately 6 mm day^{-1} for this season, and it is a season of transition (Betts et al. 2005, Marengo 2005). The value of evaporation is also low compared to NCEP/NCAR reanalysis, but the model has low interannual variability, which agrees with the reanalysis (Marengo 2005).

The moisture transport into the basin is predominantly from the east, so that the south Atlantic Ocean is the primary source of water for precipitation (Table 2). The recycling ratio is 27.2% for this season, and given that the precipitation is so large, the amount of recycled precipitation is 2 mm day^{-1} . The amount of basin evaporation that is recycled is then more than 50%. While it is difficult to intercompare the recycling ratios for different regions (e.g. length scale dependence, Eltahir and Bras, 1996), the difference in the amount of evaporation that is recycled between LBA and the MRB and MAGS is likely due to the efficiency of local water to be entrained into convective precipitation. The efficiency may be related to both the tropical environment and the model's parameterization of convective precipitation.

The LBA basin also differs from the MRB and MAGS in that the evaporation has very low interannual variability. This leads to no correlation between evaporation and precipitation (Table 3c). The model is likely evaporating near its potential rate each year. In addition, since evaporation is not changing, variations in precipitation recycling are related to changes in moisture transport. When inflowing moisture is strong (weak), the recycling is weak (strong). This is demonstrated by the anti-correlation between South Atlantic Ocean and LBA sources (Table 3). The mean analysis shows that the surface evaporative contribution to precipitation is crucial, but the large-scale atmospheric circulation governs the interannual variability of how much evaporation is recycled.

d. Bulk Diagnostic Precipitation Recycling

Bulk diagnostic estimations of precipitation recycling are straightforward derivations and solutions of basin scale water budgets using monthly mean data (Brubaker et al. 1993; Eltahir and Bras 1994, 1996; Trenberth 1998; Bosilovich and Schubert 2001; Zangvil et al 2004). For comparison, we implemented the Brubaker et al. (1993) method for each of the basins. This recycling ratio and the inflowing moisture transport (ρ_B and Q_{in} , respectively) are included in Table 1 and Table 3. The bulk recycling method tends to underestimate the WVT recycling ratio calculation. This underestimate is likely a result of the assumptions imposed on the derivation and the use of monthly mean data to make the calculation (Bosilovich and Schubert, 2002). However, the bulk recycling correlates to the WVT recycling at a very high level for each basin (Table 3). In addition, the bulk recycling calculation appears to reflect similar relationships to precipitation, evaporation and moisture transport, as the WVT recycling. This suggests that the bulk recycling calculation can represent the interannual variability of recycling as an index. This fortifies the same conclusion by Bosilovich and Schubert (2002) by adding more seasons to the calculation of the correlation, and by evaluating more basins.

5. Large-scale interactions

In order to extend the discussion of the sensitivity of precipitation recycling beyond the local basin-scale water budget, we have evaluated composite years to identify variations in the atmospheric circulation and far-field physical processes. For each basin, we have identified the 5 highest and 5 lowest seasonal values of precipitation recycling in the 50-year time series. Each of these sets of five years is combined together in a composite. The WVT precipitation recycling for each year of the composites is outside of ± 1 standard deviation of the basin mean.

a. *MacKenzie River Basin*

Figure 5 shows the mean differences between the MAGS highest and lowest precipitation recycling years. In the 1000-500hPa Thickness field, high values over the region west of MAGS, and low anomalies over the rest of North America occur when recycling is high. Coincident with the height features is a southward shift of the zonal moisture transport (Figure 5b). The local positive evaporation anomaly in MAGS is not persistent across the basin. There is a reduction of evaporation in the Pacific Ocean off the west coast of the United States, but this is likely of secondary importance compared to the moisture transport anomaly. West of MAGS through Alaska, the surface temperatures are warm (Figure 5d), and the soil moisture in the top layers is dry (not shown). In general, the soil moisture anomaly is positive for the interior of MAGS when recycling is high, but the driving feature is the zonal moisture transport.

b. *Mississippi River Basin*

In the MRB, high recycling years are characterized by low heights (and 1000-500 hPa thicknesses) over the continental United States (Figure 6a). The circulation anomaly coincides with a reduction in the northward transport of moisture by the low level jet (Figure 6b) and a reduction in the tropical easterly transport of moisture across the Gulf of Mexico (not shown). In the high recycling years, there is ample soil moisture and the evaporation in the basin is generally strong. There is a cold anomaly across the basin, but it extends beyond the basin and the increased evaporation anomaly. This does not indicate that the low level jet is not important to the water cycle of the region. Rather, the low level jet is the dynamical trigger for convection, and the occurrence of high evaporation enhances the resulting precipitation.

In high recycling years, SSTs in the equatorial Pacific Ocean are noticeably warm (Figure 6d). In evaluating extreme events in the United States climatology, Trenberth and Guillemot (1996) show that the tropical SSTs had some influence on the MJJ large scale

circulation including the low-level jet, where warm (cold) tropical Pacific SSTs were related to the 1993 flooding precipitation (1988 drought and heat wave). We computed the correlations of the MJJ precipitation and recycling with the Nino 1+2 region (0° – 10° S, 90° – 80° W) SST anomaly in the model. The correlations are positive but small (0.38 for precipitation, 0.37 for recycling ratio). There are occasions when the precipitation recycling is high, but the equatorial Pacific SSTs are cold. This is likely related to the complexity of the teleconnections, and also the memory of the land surface soil moisture, where deep soil moisture anomalies could persist for some time, affecting the surface evaporation and recycling.

c. Amazon River Basin

When recycling is high in the LBA basin, the inflow of moisture from the east is reduced (Table 3). The zonal moisture transport anomaly that is associated with this extends from the southern Atlantic Ocean into the equatorial Pacific Ocean (Figure 7a) for the extreme (high and low) recycling years. The precipitation anomaly for high LBA recycling is also positive (Figure 7b), even with less moisture inflow. The precipitation across the Atlantic convergence zone is generally increased for high LBA recycling. Figure 7c is included to contrast the MRB recycling dependency on evaporation with the LBA. The SST anomaly shows cold temperatures in the equatorial Pacific Ocean for high precipitation recycling years (Figure 7d). These cold temperatures are likely contributing to the weakening of the zonal moisture transport.

In general, SSTs are increasing during these 50 years of simulation, which leads to a general decreasing trend of global precipitation over land (e.g. Bosilovich et al. 2005). Here, we evaluated the MRB and MAGS for trends in the water cycle, and there was no statistical significance in these basins. However, the LBA precipitation decreases over the 50 years (-0.1 mm day⁻¹ per decade of annual average precipitation). This is, in part, related to the reduction of recycling in time (Figure 8). The relationship discussed earlier between recycling and moisture

transport is apparent in the time series. The recycling ratio is decreasing by -2.4% and the easterly moisture transport increases by 0.83 mm day^{-1} over the 50 years. The trends are responding to the SST forcing. Changes in leaf area index and vegetation cover are not included, but might also affect the recycling and feedback.

6. Summary and conclusions

Precipitation recycling is an important process in the water budget and land atmosphere interactions of a large river basin. However, the mechanisms driving the interactions are not linear, and may vary among basins. Here, we evaluate a long AGCM simulation of the water cycle in three river basins with distinct regional differences; MAGS, MRB and LBA. In addition to the basin averaged water budget terms, we also include analysis of water sources and precipitation recycling from water vapor tracers and a bulk diagnostic precipitation recycling method. The simulation used the observed SST from the Hadley Centre to prescribe the ocean surface forcing, but no other prescribed time varying data (e.g. vegetation, carbon dioxide or aerosols). The model forcing and configuration will be improved in forthcoming Climate of the 20th Century experiments (Folland et al, 2002).

Given the definition of precipitation recycling: “the contribution of local evaporation to local precipitation” (Eltahir and Bras, 1996), one might assume that the precipitation recycling is a sole function of evaporation. Indeed, without evaporation, there would be no precipitation recycling, and the annual cycle of precipitation recycling tracks evaporation (Bosilovich and Schubert, 2001). While most studies include a discussion of the moisture transport (Brubaker et al. 1993; Eltahir and Bras, 1996), in some regions the interannual variability of the precipitation recycling is strongly related to the interannual variability of the moisture transport (e.g. MAGS and LBA). In the MRB, there was some concurrent variability of the moisture transport with

precipitation recycling, but the sensitivity to evaporation is much larger. This may be expected, as the region has been identified as an area of enhanced land atmosphere coupling in many models (Koster et al. 2004).

One result that is important for future studies is the strong correlation between recycling ratios calculated from the WVT method and the bulk diagnostic method (Brubaker et al. 1993). The WVT recycling ratios are diagnosed from passive tracers that are predicted forward in time at the model time step. The WVTs experience the diurnal cycle, individual convective events and synoptic storm systems, while taking up modest computing resources. The bulk diagnostic recycling is computed with monthly mean water budget data after the simulation is completed. The bulk recycling variability in coupled ocean atmosphere simulations or reanalyses will provide useful information on the local coupling. The weakness of this method is that it cannot account for sources and destinations of water vapor other than the recycling.

The current WVT method also has some weaknesses. The source regions are defined at the beginning of the simulation. If, at a later date, a new source region were required, the simulation would have to be performed again. Also, while large-scale sources can be identified (e.g. Pacific Ocean), the regional sources geographic locations cannot be identified more specifically. Ideally, if tracer sources could be identified at specific grid points, the WVT method could be used to identify both forward and backward tracing of water.

Acknowledgments

We appreciate the efforts of Peter Troch, Eric Wood and the organizing committee of the Catchment Area Hydrological Modeling and Data Assimilation (CAHMDA-II) workshop. The

discussions over poster sessions at the meeting were particularly useful in finalizing this manuscript. This work was supported by the NASA Global Water and Energy Cycles program.

7. References

- Adler et al., 2003 The Version-2 Global Precipitation Climatology Project (GPCP) Monthly Precipitation Analysis (1979–Present). *J. Hydromet.*, **4**, 1147-1167.
- Betts, A. K., 2004: Understanding Hydrometeorology Using Global Models. *Bull. Amer. Meteor. Soc.*, **85**, 1673-1688
- Betts, A. K., J. H. Ball, and P. Viterbo, 2003: Evaluation of the ERA-40 surface water budget and surface temperature for the Mackenzie River basin. *J. Hydromet.*, **4**, 1194-1211.
- Betts, A. K., J. H. Ball, P. Viterbo, A. Dai and J Marengo, 2005: Hydrometeorology of the Amazon in ERA40. *J. Hydromet.* Accepted for publication.
- Bonan G. B., K. W. Oleson, M. Vertenstein, S. Levis, X. Zeng, Y. Dai, R. E. Dickinson and Z.-L. Yang, 2002: The Land Surface Climatology of the Community Land Model Coupled to the NCAR Community Climate Model. *J. Climate*, **15**, 3123–3149.
- Bosilovich, M. G., 2002: On the Vertical Distribution of Local and Remote Sources of Water for Precipitation, *Meteorol. Atmos. Phys.*, **80**, 31-41.
- Bosilovich, M. G., and S. D. Schubert, 2001: Precipitation recycling in the GEOS-1 data assimilation system over the central United States, *J. Hydromet.*, **2**, 26 – 35.
- Bosilovich, M. G. and S. D. Schubert, 2002: Water vapor tracers as diagnostics of the regional hydrologic cycle, *J. Hydromet.*, **3**, 149-165.
- Bosilovich, M. G., Y. C. Sud, S. D. Schubert and G. K. Walker, 2003: Numerical simulation of the North American monsoon water sources. *J. Geophys. Res.*, **108**(D16), 8614, doi:10.1029/2002JD003095.
- Bosilovich, M. G., S.D. Schubert, and G. K. Walker, 2004: Global changes of the water cycle intensity. Accepted to Journal of Climate.

- Brubaker, K., D. Entekahabi, and P. Eagleson, 1993: Estimation of precipitation recycling. *J. Climate*, **6**, 1077–1089.
- Brubaker, K. L., P. A. Dirmeyer, A. Sudradjat, B. S. Levy and F. Bernal, 2001: A 36-year climatological description of the evaporative sources of warm-season precipitation in the Mississippi River Basin. *J. Hydromet.*, **2**, 537-557.
- Collins, W. D., J. J. Hack, B. A. Boville, P. J. Rasch, D. L. Williamson, J. T. Kiehl, B. Brieglib, C. Bitz, S.-J. Lin, and R. B. Rood, 2004: Description of the NCAR Community Atmosphere Model (CAM2), NCAR/TN-464+STR, 190 pp., Natl. Cent. For Atmos. Res., Boulder, Colo.
- Dai, Y. and Co-Authors, 2003: The Common Land Model (CLM). *Bull. Amer. Met. Soc.*, **84**, 1013-1023.
- Dirmeyer, P. A., and K. L. Brubaker, 1999: Contrasting evaporative moisture sources during the drought of 1988 and the flood of 1993. *J. Geophys. Res.*, **104**, 19 383–19 398.
- Eltahir, E. A. B., and R. L. Bras, 1994: Precipitation recycling in the Amazon basin. *Quart. J. Roy. Meteor. Soc.*, **120**, 861–880.
- Eltahir, E. A. B., and R. L. Bras, 1996: Precipitation recycling. *Rev. Geophys.*, **34**, 367–378
- Folland, C., J. Shukla, J. Kinter, and M. Rodwell, 2002: The Climate of the Twentieth Century Project. CLIVAR Exchanges News Letter, v. 7, no. 2, 37-39.
- Hack, J. J., 1994: Parameterization of moist convection in the National Center for Atmospheric Research Community Climate Model (CCM2). *J. Geophys. Res.*, **99**, 5551-5568.
- Kiehl, J. T., J. J. Hack, G. B. Bonan, B. A. Boville, D. L. Williamson, and P. J. Rasch, 1998: The National Center for Atmospheric Research Community Climate Model (CCM3), *J. Clim.*, **11**, 1131-1149.

- Koster, R. D., P. A. Dirmeyer and co-authors, 2004: Regions of strong coupling between soil moisture and precipitation. *Science*, **305**, 1138-1140.
- Lettau, H., K. Lettau and L.C.B. Molion, 1979: Amazonia's Hydrologic Cycle and the Role of Atmospheric Recycling in Assessing Deforestation Effects. *Mon. Wea. Rev.*, **107**, 227–238.
- Lin, S.-J., 2003: A "vertically Lagrangian" finite-volume dynamical core for global models. *Mon. Wea. Rev.*, **132**, 2293-2307.
- Lin, S.-J., and R. B. Rood, 1997: An explicit flux-form semi-Lagrangian shallow-water model on the sphere, *Q. J. Roy. Meteor. Soc.*, **123**, 2477 – 2498.
- MacKay, M. D., F. Seglenciks, D. Verseghe, E. D. Soulis, K. R. Snelgrove, A. Walker and, K. Szeto, 2003: Modeling Mackenzie Basin Surface Water Balance during CAGES with the Canadian Regional Climate Model. *J. Hydromet.*, **4**, 748-767.
- Marengo, J., 2004: Interdecadal variability and trends of rainfall across the Amazon basin. *Theor. Appl. Climatol.*, **78**, 79–96. DOI 10.1007/s00704-004-0045-8.
- Marengo, J., 2005: Characteristics and spatio-temporal variability of the Amazon River Basin Water Budget, *Climate Dynamics*, DOI: 10.1007/s00382-004-0461-6.
- Oleson, K. W., Y. Dai, G. Bonan and co-authors, 2004: Technical Description of the Community Land Model (CLM), NCAR/TN-461+STR, 173 pp., Natl. Cent. For Atmos. Res., Boulder, Colo.
- Rayner, N.A., Horton, E.B., Parker, D.E., Folland, C.K., and Hackett, R.B., 1996: Version 2.2 of the global sea-ice and sea surface temperature data set, 1903-1994. Climate Research Technical Note No. 74, The Met Office.
- Rayner, N. A., D. E. Parker, E. B. Horton, C. K. Folland, L. V. Alexander, D. P. Rowell, E. C. Kent, and A. Kaplan, 2003: Global analyses of sea surface temperature, sea ice, and night

- marine air temperature since the late nineteenth century, *J. Geophys. Res.*, **108(D14)**, 4407, doi:10.1029/2002JD002670.
- Roads, J. O., M. Kanamitsu and R. Stewart, 2002: CSE Water and Energy Budgets in the NCEP–DOE Reanalysis II, *J. Hydromet.*, **3**, 227-248.
- Schubert, S. D., M. J. Suarez, P. J. Pegion, R. D. Koster and J. T. Bacmeister, 2004a: Causes of long-term drought in the United States great plains. *J. Climate*, **17**, 485-503.
- Schubert, S. D., M. J. Suarez, P. J. Pegion, R. D. Koster, J. T. Bacmeister, 2004b: On the cause of the 1930s Dust Bowl. *Science*, **303**, 1855-1859.
- Simpson, J. J., J. S. Berg, C. J. Koblinsky, G. L. Hufford, and B. Beckley, 2001: The NVAP global water vapor data set: Independent cross comparison and multi year variability, *Remote Sens. Environ.*, **76**, 112– 129, 2001.
- Stohl A. and P. James, 2004: A Lagrangian Analysis of the Atmospheric Branch of the Global Water Cycle. Part I: Method Description, Validation, and Demonstration for the August 2002 Flooding in Central Europe. *J. Hydromet.*, **5**, 656-678.
- Szeto, K. K., 2002: Moisture Recycling over the Mackenzie Basin. *Atmos.-Ocean*, **40** 181–197.
- Trenberth, K. E., 1998: Atmospheric moisture residence times and cycling: Implications for rainfall rates and climate change. *Climatic Change*, **39**, 667-694.
- Trenberth, K. E. and C. J. Guillemot, 1996: Physical Processes Involved in the 1988 Drought and 1993 Floods in North America. *J. Climate*, **9**, 1288–1298.
- Trenberth, K. E., A. Dai, R. M. Rasmussen, D. B. Parsons, 2003: The Changing Character of Precipitation. *Bull. Amer. Meteor. Soc.*, **84**, 1205-1217.
- Yoshimura, K., T. Oki, N. Ohte and S. Kanae, 2004: Colored moisture analysis estimates of variations in 1998 Asian monsoon water sources. *J. Meteorol. Soc. Japan*, **82**, 1315-1329.

- Zangvil, A., D. H. Portis, and P. J. Lamb, 2004: Investigation of the Large-Scale Atmospheric Moisture Field over the Midwestern United States in Relation to Summer Precipitation. Part II: Recycling of Local Evapotranspiration and Association with Soil Moisture and Crop Yields. *J. Clim.*, **17**, 3283-3301.
- Zeng, X., M. Shaikh, Y. Dai, R. E. Dickinson, and R. Myneni, 2002: Coupling of the Common Land Model to the NCAR Community Land Model. *J. Climate*, **15**, 1832-1854.
- Zhang, G. J., and N. A. McFarlane, 1995: Sensitivity of climate simulation to the parameterization of cumulus convection in the Canadian Climate Centre general circulation model. *Atmos.-Ocean*, **33**, 407-446.

8. List of Tables

Table 1 Maximum recycling season time means, area averaged over each basin, MAGS, MRB and LBA. The variables are P, precipitation; E, evaporation; TPW, total precipitable water; QV, vertically integrated moisture transport at each boundary facing north (N), south (S), east (E) and west (W); ρ , recycling ratio computed from the WVT and Brubaker et al. (1993) Bulk (B) methods and the inflowing moisture for the Brubaker (1993) method (Q_{in} is the line integrated inward transport of water for this method). All units are mm day^{-1} , except for TPW (mm) and recycling ratios (percent of total precipitation).

Table 2 Major precipitation source regions for each basin, MAGS, MRB and LBA and the percentage of total precipitation during the 3 month season of maximum precipitation recycling (MJJ for MAGS and MRB, and OND for LBA). Region acronyms are identified in Figure 1.

Table 3 Correlations of water cycle variables during the season of maximum precipitation recycling for (a) MAGS, (b) MRB and (c) LBA. The variables are defined in Table 1. The percentage of total precipitation from major source regions, as well as precipitation recycling, is also included. In (b), *Trop Atl* indicates the sum of all sources from the tropical Atlantic Ocean (NTA, STA, CAR and GOM). Values 0.5 or greater are bold, values -0.5 or less are underscored.

9. Tables

Table 1 Maximum recycling season time means, area averaged over each basin, MAGS, MRB and LBA. The variables are P, precipitation; E, evaporation; TPW, total precipitable water; QV, vertically integrated moisture transport at each boundary facing north (N), south (S), east (E) and west (W); ρ , recycling ratio computed from the WVT and Brubaker et al. (1993) Bulk (B) methods and the inflowing moisture for the Brubaker (1993) method (Q_{in} is the line integrated inward transport of water for this method). All units are mm day^{-1} , except for TPW (mm) and recycling ratios (percent of total precipitation).

	MAGS	MRB	LBA
P	1.9	2.6	7.3
E	2.1	2.7	3.8
TPW	13.6	23.2	43.8
QV_W	5.0	1.8	-2.7
QV_E	-5.7	-5.9	6.8
QV_S	0.7	5.2	-2.1
QV_N	-0.1	-1.2	1.6
ρ_{WVT}	19.6	23.4	27.2
ρ_B	13.7	14.4	17.5
Q_{in}	6.8	8.1	9.0

Table 2 Major precipitation source regions for each basin, MAGS, MRB and LBA and the percentage of total precipitation during the 3 month season of maximum precipitation recycling (MJJ for MAGS and MRB, and OND for LBA). Region acronyms are identified in Figure 1.

Rank	MAGS	MRB	LBA
1	NPO (36.6)	MRB (23.4)	SAO (43.4)
2	MAGS (19.6)	US (16.1)	LBA (27.2)
3	CAN (17.7)	NPO (15.5)	SAM (9.2)
4	ASA (14.9)	NTA (13.9)	STA (5.1)
5	POL (2.9)	GOM (8.9)	AFR (4.8)
6	US+MRB (2.9)	CAR (5.3)	INO (3.8)

Table 3 Correlations of water cycle variables during the season of maximum precipitation

recycling for (a) MAGS, (b) MRB and (c) LBA. The variables are defined in Table 1.

The percentage of total precipitation from major source regions, as well as precipitation

recycling, is also included. In (b), *Trop Atl* indicates the sum of all sources from the

tropical Atlantic Ocean (NTA, STA, CAR and GOM). Values 0.5 or greater are bold,

values -0.5 or less are underscored.

a

MAGS	<i>P</i>	<i>E</i>	<i>P-E</i>	<i>TPW</i>	MAGS	NPO	Asia	<i>QV_w</i>	<i>QV_E</i>	<i>QV_S</i>	<i>QV_N</i>	ρ_B
E	0.50	1.00										
P-E	0.81	-0.10	1.00									
TPW	0.46	0.45	0.22	1.00								
MAGS	0.53	0.31	0.40	0.29	1.00							
NPO	<u>-0.55</u>	-0.18	<u>-0.50</u>	-0.34	<u>-0.58</u>	1.00						
Asia	<u>-0.69</u>	-0.33	<u>-0.57</u>	-0.32	<u>-0.63</u>	0.41	1.00					
<i>QV_w</i>	<u>-0.51</u>	-0.04	<u>-0.56</u>	-0.42	<u>-0.67</u>	0.61	0.65	1.00				
<i>QV_E</i>	0.59	0.01	0.67	0.49	0.61	<u>-0.52</u>	<u>-0.60</u>	<u>-0.83</u>	1.00			
<i>QV_S</i>	0.01	0.34	-0.21	0.07	-0.03	-0.01	0.07	0.04	-0.25	1.00		
<i>QV_N</i>	-0.17	-0.27	-0.01	-0.31	-0.02	-0.04	-0.04	-0.10	-0.26	-0.48	1.00	
ρ_B	0.63	0.22	0.58	0.44	0.71	-0.45	<u>-0.60</u>	<u>-0.76</u>	0.81	-0.05	-0.21	1.00
<i>Q_{in}</i>	<u>-0.55</u>	0.04	<u>-0.66</u>	-0.34	<u>-0.61</u>	0.41	0.54	0.76	<u>-0.85</u>	0.17	0.17	<u>-0.94</u>

b

MRB	<i>P</i>	<i>E</i>	<i>P-E</i>	<i>TPW</i>	MRB	NPO	<i>Trop Atl</i>	<i>QV_w</i>	<i>QV_E</i>	<i>QV_S</i>	<i>QV_N</i>	ρ_B
E	0.96	1.00										
P-E	0.83	0.64	1.00									
TPW	0.57	0.55	0.46	1.00								
MRB	0.87	0.88	0.61	0.41	1.00							
NPO	<u>-0.54</u>	<u>-0.54</u>	-0.41	-0.43	<u>-0.58</u>	1.00						
<i>Trop Atl</i>	-0.36	-0.36	-0.27	0.25	-0.48	-0.03	1.00					
<i>QV_w</i>	0.31	0.31	0.22	-0.13	0.19	0.32	-0.41	1.00				
<i>QV_E</i>	-0.17	-0.12	-0.21	-0.03	0.04	-0.29	-0.01	<u>-0.69</u>	1.00			
<i>QV_S</i>	0.40	0.32	0.45	0.64	0.05	-0.19	0.40	0.09	<u>-0.54</u>	1.00		
<i>QV_N</i>	-0.16	-0.21	-0.03	<u>-0.54</u>	-0.04	0.35	-0.34	0.39	<u>-0.51</u>	-0.35	1.00	
ρ_B	0.73	0.79	0.43	0.20	0.87	-0.47	<u>-0.59</u>	0.17	0.27	-0.26	-0.05	1.00
<i>Q_{in}</i>	0.28	0.24	0.28	0.49	-0.06	-0.06	0.38	0.20	<u>-0.60</u>	0.90	-0.24	-0.41

c

LBA	<i>P</i>	<i>E</i>	<i>P-E</i>	<i>TPW</i>	LBA	SAO	STA	<i>QV_w</i>	<i>QV_E</i>	<i>QV_S</i>	<i>QV_N</i>	ρ_B
E	-0.03	1.00										
P-E	0.99	-0.18	1.00									
TPW	0.62	-0.06	0.62	1.00								
LBA	0.23	0.27	0.18	-0.04	1.00							
SAO	-0.48	0.08	-0.49	-0.31	<u>-0.64</u>	1.00						
STA	0.19	-0.03	0.19	0.33	-0.33	-0.16	1.00					
<i>QV_w</i>	0.62	-0.10	0.62	0.21	0.63	<u>-0.72</u>	-0.10	1.00				
<i>QV_E</i>	-0.37	0.08	-0.38	-0.22	<u>-0.77</u>	0.85	-0.04	<u>-0.75</u>	1.00			
<i>QV_S</i>	0.45	-0.08	0.45	0.26	0.42	-0.40	-0.07	0.19	-0.50	1.00		
<i>QV_N</i>	0.42	-0.13	0.44	0.65	-0.14	-0.28	0.64	-0.06	-0.24	0.24	1.00	
ρ_B	0.05	0.34	0.00	-0.30	0.87	-0.48	-0.37	0.58	<u>-0.68</u>	0.35	-0.41	1.00
<i>Q_{in}</i>	-0.06	0.00	-0.06	0.30	<u>-0.83</u>	0.54	0.38	<u>-0.66</u>	0.75	-0.38	0.39	<u>-0.94</u>

10. List of Figures

Figure 1 Map of source regions for water vapor tracers (WVTs), where each color indicates a different evaporative source region. The regions are MAGS, MacKenzie Area GEWEX Study; MRB, Mississippi River Basin; LBA, Large-scale Biosphere Atmosphere experiment for the Amazon; NPO, North Pacific Ocean; SAO, South Atlantic Ocean; STA, South Tropical Atlantic Ocean; NTA, North Tropical Atlantic Ocean; CAR, Caribbean Sea; GOM, Gulf of Mexico; AFR; Africa; ASA, Asia; CAN, Canada and SAM, South America. The land area to the east and west of MRB, including Mexico are included in a WVT called US.

Figure 2 Seasonal intercomparison of simulated (fvGCM) precipitation with the merged precipitation observations from the Global Precipitation Climatology Project (GPCP; Adler et al. 2003). The seasons were averaged for December 1979 through November 1997, where the model and observation data coincide. The seasons are December-February (DJF), a and b; March – May (MAM), c and d; June – August (JJA), e and f; and September – November (SON), g and h. The units are mm day^{-1} .

Figure 3 As in Figure 2, except for fvGCM simulated Total Precipitable Water (TPW) and the NVAP observed data (Simpson et al., 2001). The seasons are averaged for December 1988 through November 1999, where the model and observations coincide. The units are mm of water integrated in the atmospheric column.

Figure 4 Mean annual cycle of basin averaged water sources for MAGS, MRB and LBA. The colors are identical to the regions in Figure 1. Note that the major oceanic sources are scaled on the right axis. The units are percent of total precipitation.

Figure 5 Mean differences between the five highest and five lowest precipitation recycling years (MJJ) for the MAGS basin of (a) 500 –1000 hPa Thickness (m), (b) vertically integrated zonal moisture transport ($\text{ms}^{-1})(\text{g kg}^{-1})$, (c) Evaporation (mm day^{-1}), and (d) surface temperature (K). The black contours show the statistically significant differences (at the 5% and 10% level). The MAGS basin grid points are outlined.

Figure 6 As in Figure 5, except for the MRB. The moisture transport (b) is for the meridional component.

Figure 7 Mean differences between the five highest and five lowest precipitation recycling years (OND) for the LBA basin of (a) vertically integrated zonal moisture transport ($(\text{ms}^{-1})(\text{g kg}^{-1})$), (b) precipitation (mm day^{-1}) (c) evaporation (mm day^{-1}), and (d) surface temperature (K). The black contours show the statistically significant differences (at the 5% and 10% level). The LBA basin grid points are outlined.

Figure 8 Time series of OND LBA precipitation recycling ratio (black dots, left axis) and zonal moisture transport from the east (crosses, right axis).

11. Figures

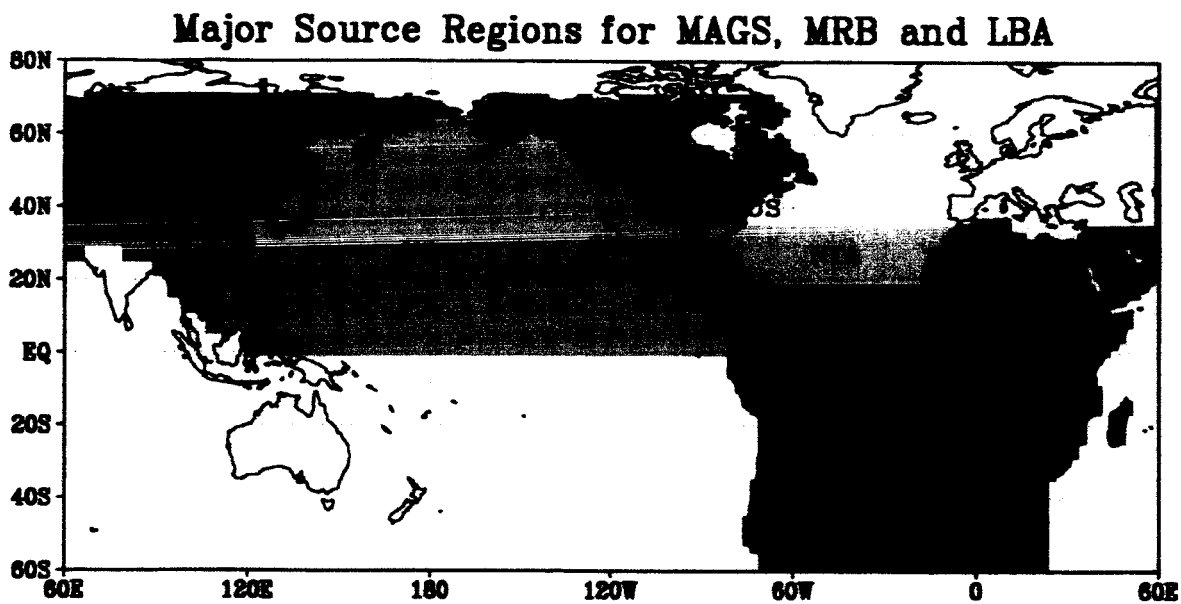


Figure 1

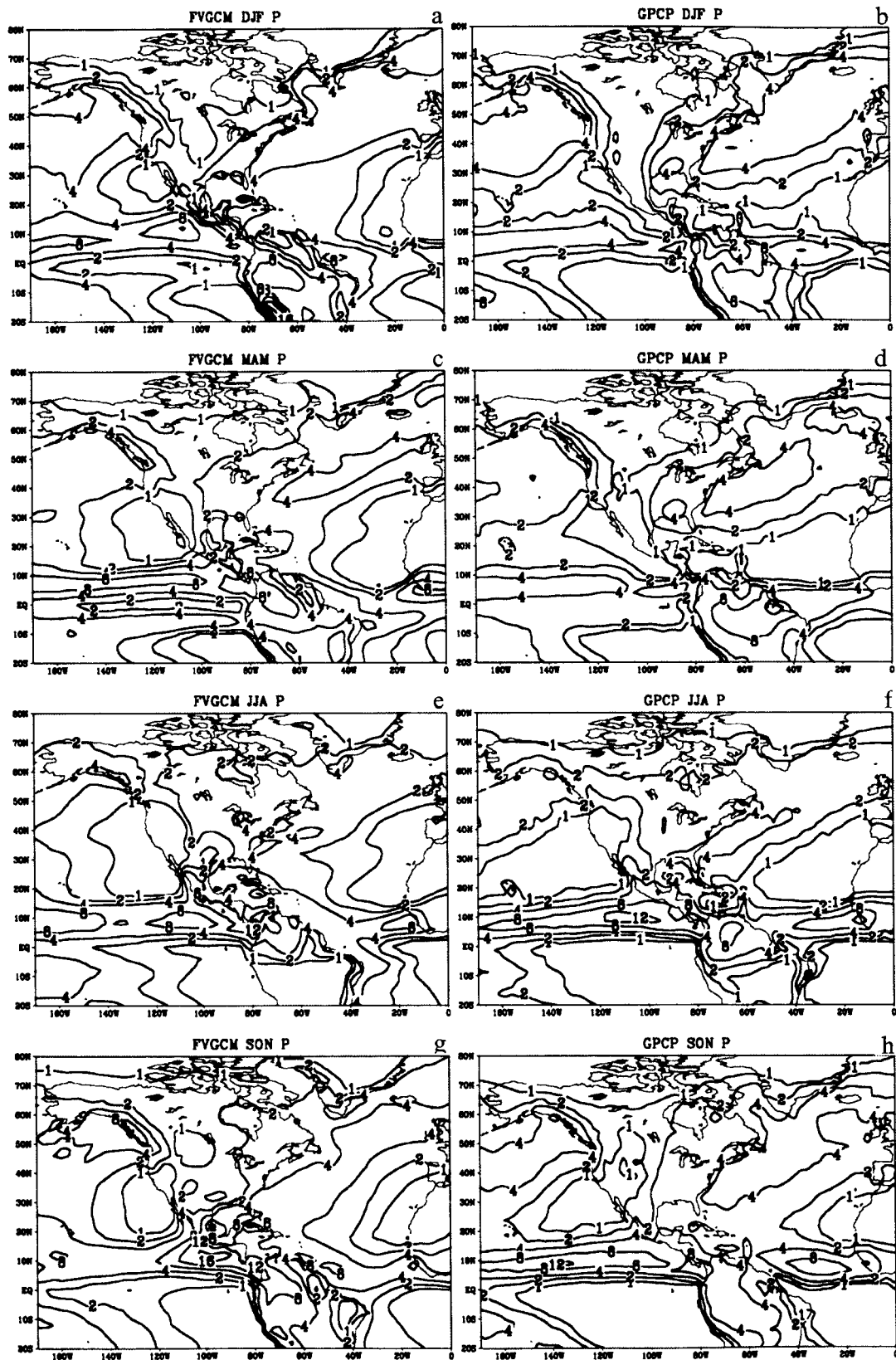


Figure 2

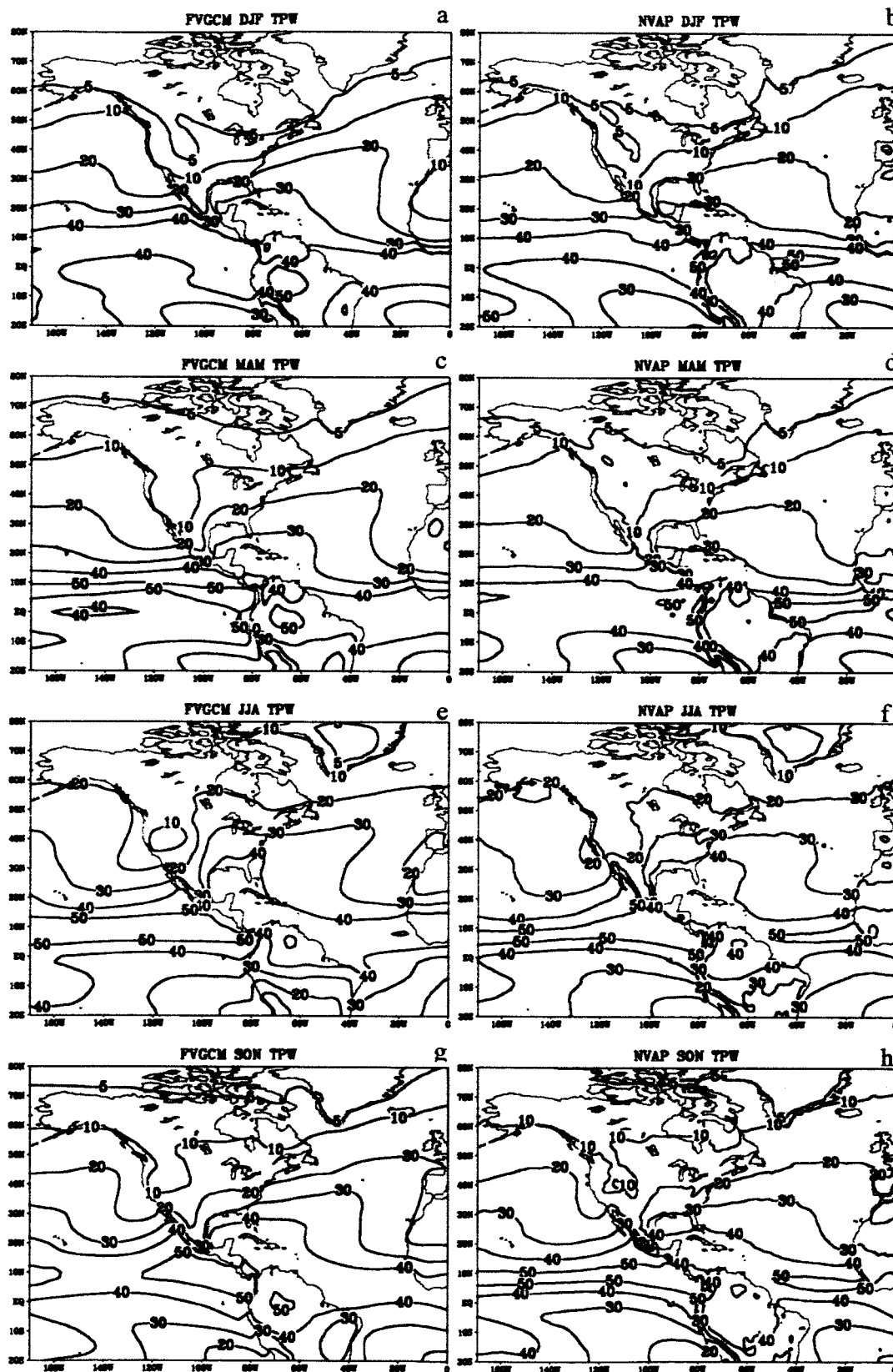


Figure 3

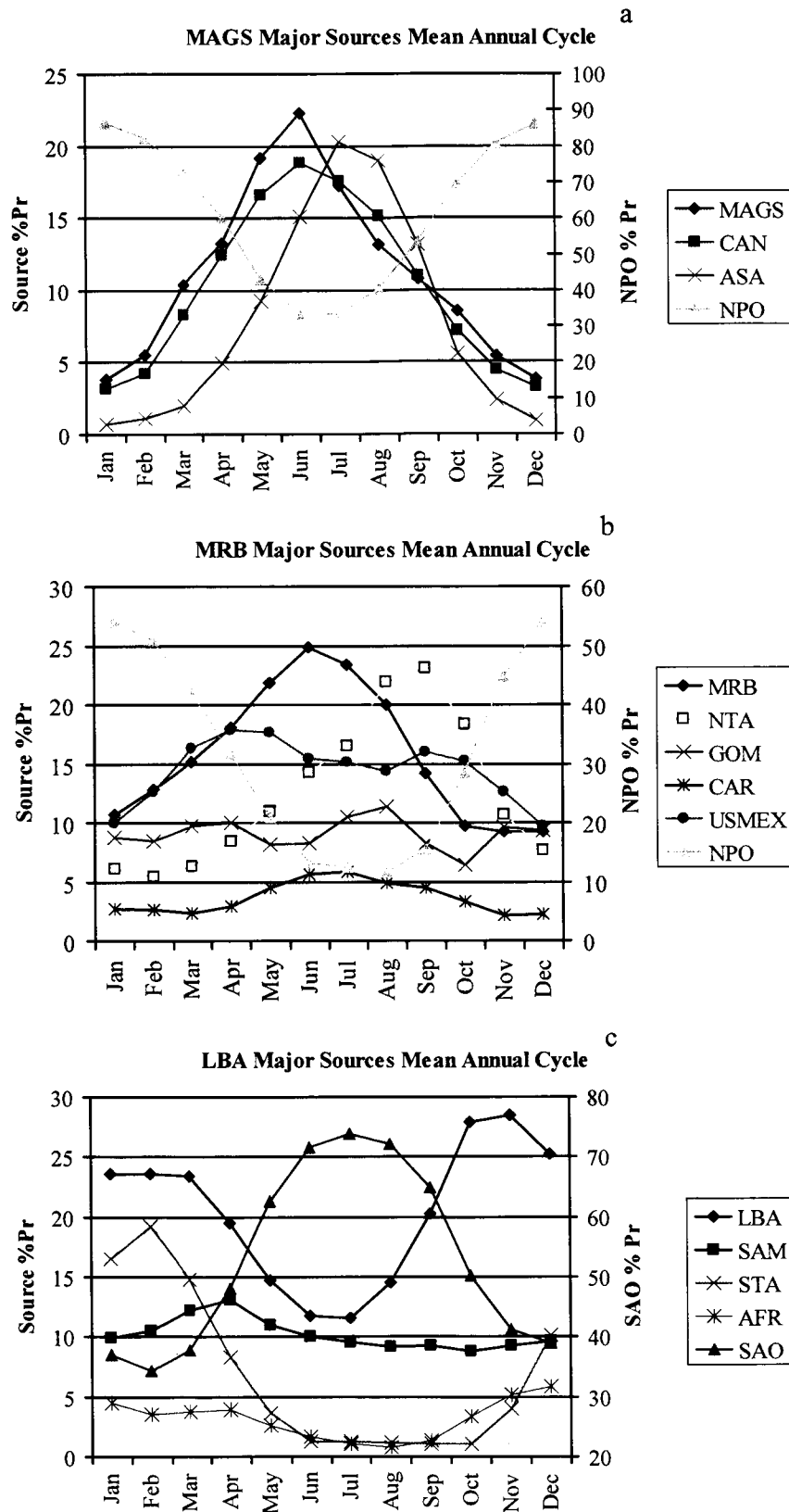


Figure 4

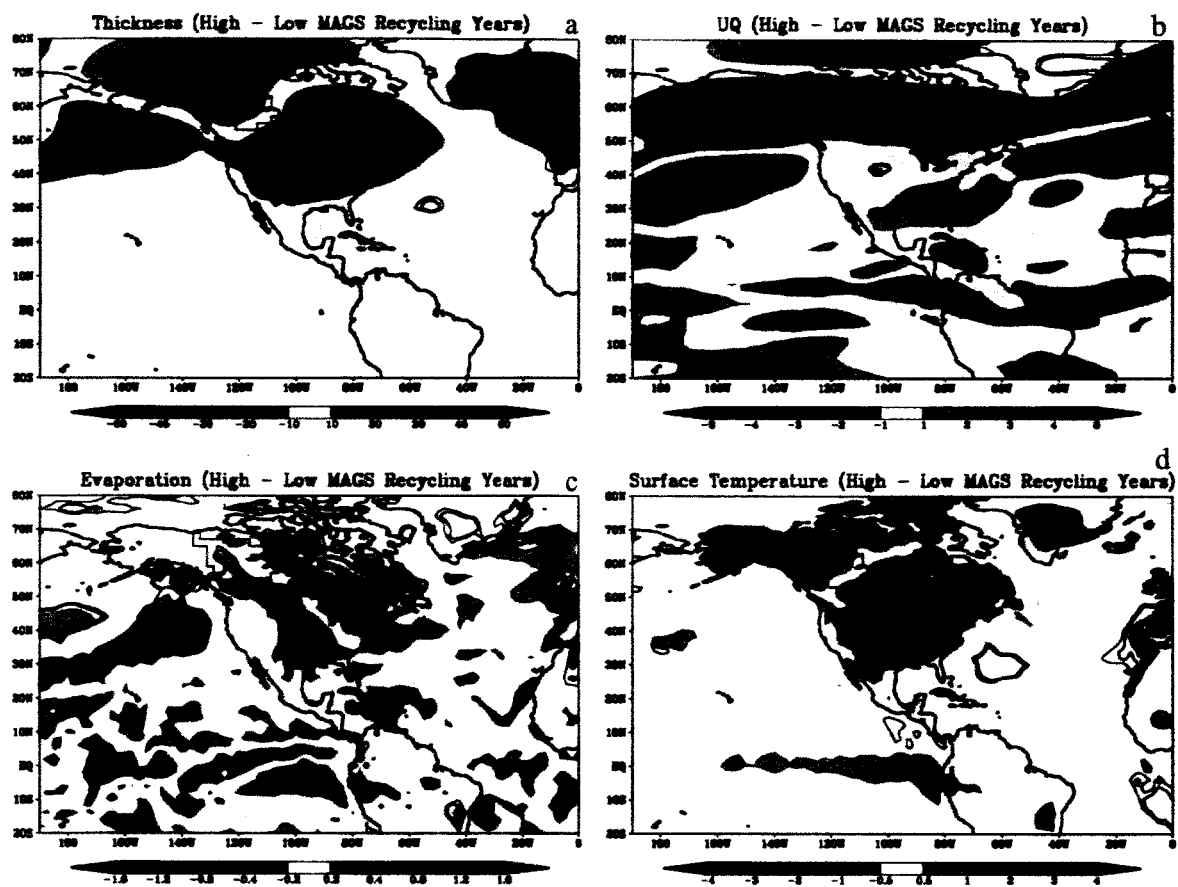


Figure 5

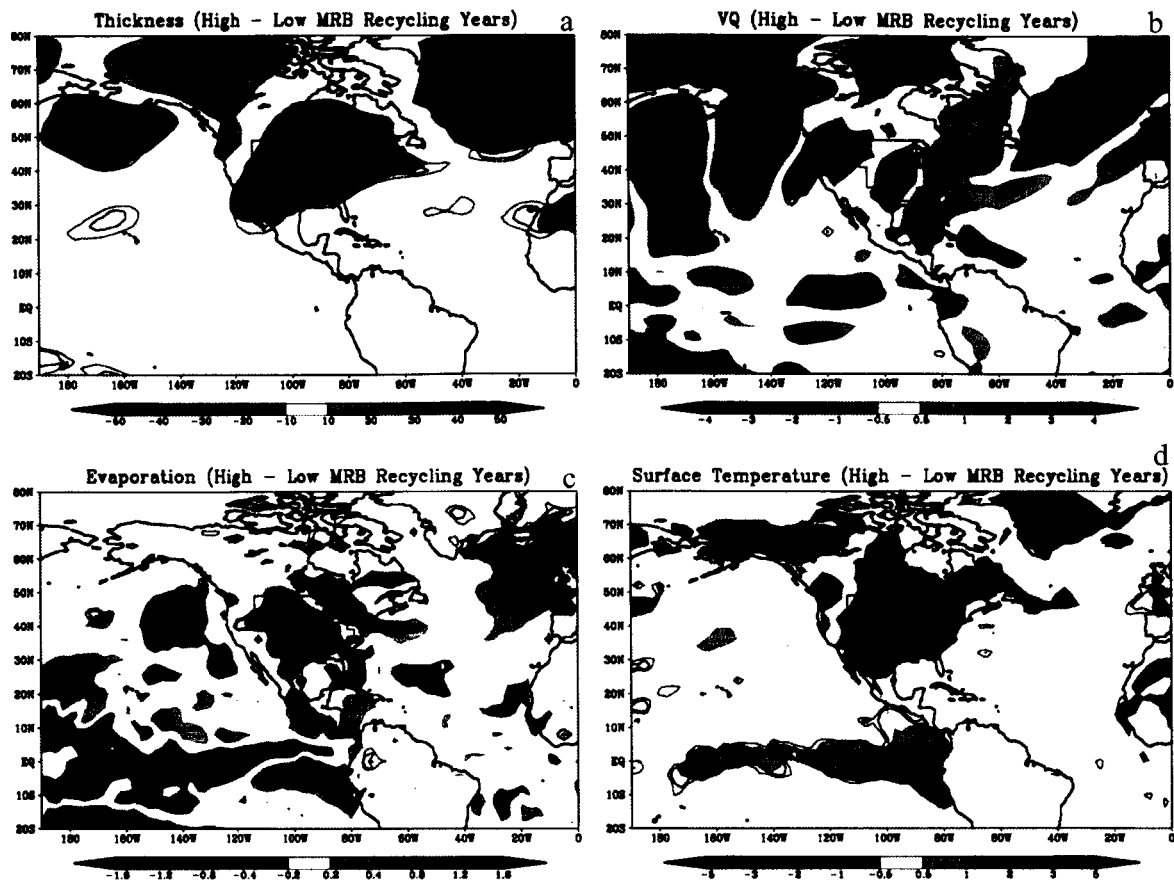


Figure 6

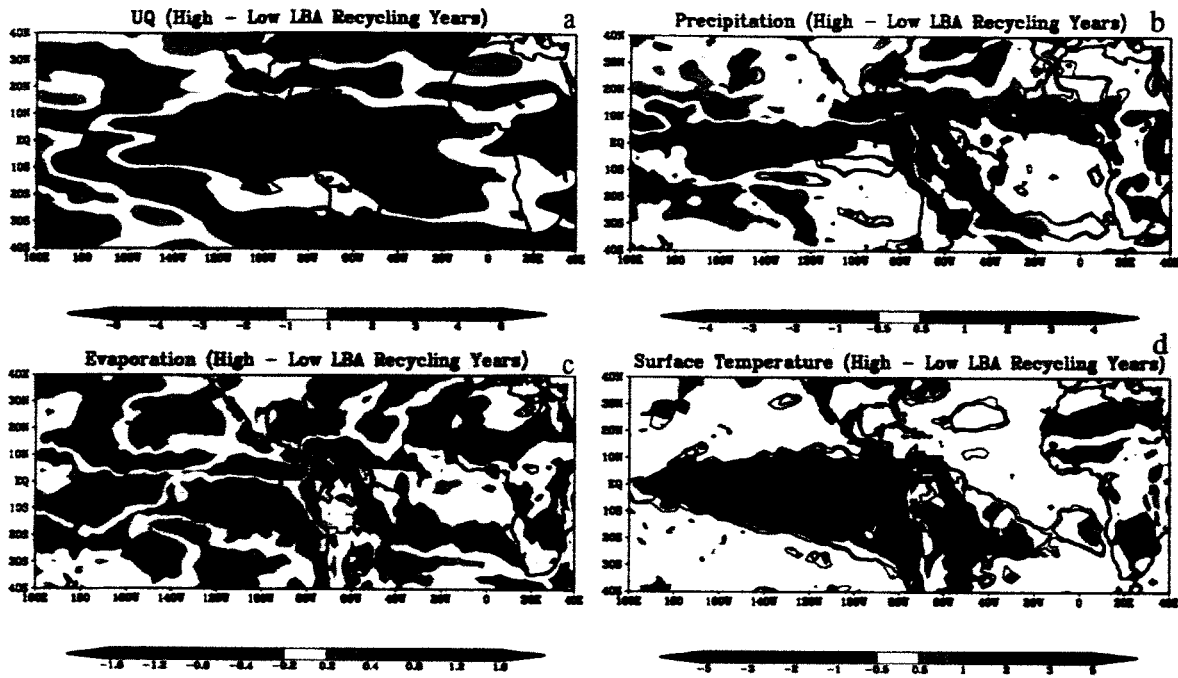


Figure 7

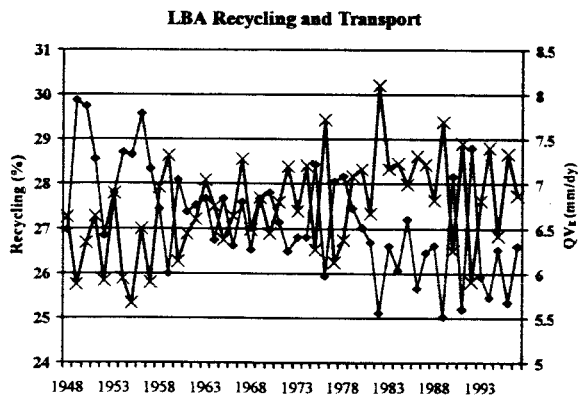


Figure 8

Simulation of Water Sources and Precipitation Recycling for the Mac Kenzie, Mississippi and Amazon River Basins

Journal of Hydrometeorology, AMS Journals
(ISSN 1525-755X), Vol. 5, 2004

ABSTRACT

An atmospheric general circulation model simulation for 1948-1997 of the water budgets for the MacKenzie, Mississippi and Amazon River basins is presented. In addition to the water budget, we include passive tracers to identify the geographic sources of water for the basins, and the analysis focuses on the mechanisms contributing to precipitation recycling in each basin. While each basin's precipitation recycling has a strong dependency on evaporation during the mean annual cycle, the interannual variability of the recycling shows important relationships with the atmospheric circulation. The MacKenzie River basin has only a weak interannual dependency on evaporation, where the variations in zonal moisture transport from the Pacific Ocean can affect the basin water cycle. On the other hand, the Mississippi River basin has strong interannual dependencies on evaporation. While the precipitation recycling weakens with increased low level jet intensity, the evaporation variations exert stronger influence in providing water vapor for convective precipitation at the convective cloud base. High precipitation recycling is also found to be partly connected to warm SSTs in the tropical Pacific Ocean. The Amazon River basin evaporation exhibits small interannual variations, so that the interannual variations of precipitation recycling are related to atmospheric moisture transport from the tropical south Atlantic Ocean. Increasing SSTs over the 50-year period are causing increased easterly transport across the basin. As moisture transport increases, the Amazon precipitation recycling decreases (without real time varying vegetation changes). In addition, precipitation recycling from a bulk diagnostic method is compared to the passive tracer method used in the analysis. While the mean values are different, the interannual variations are comparable between each method. The methods also exhibit similar relationships to the terms of the basin scale water budgets.